

# Electromagnetic Time Reversal Method to Locate Partial Discharges in Power Networks Using 1D TLM Modelling

A. Ragusa<sup>1</sup>, Member, IEEE, H. Sasse, A. Duffy<sup>1</sup>, Fellow, IEEE, F. Rachidi<sup>2</sup>, Fellow, IEEE, and M. Rubinstein, Fellow, IEEE

**Abstract**—This letter sets out to describe the first results of the design process that will lead to a new on-line partial discharge location method based on Electromagnetic Time Reversal theory and using the Transmission Line-Matrix method. A description of the basic steps of the method under design is given together with the modeling procedure used to describe time inverted signal propagation. Finally, the ability of the method to locate partial discharges on power cables both using two observation points and a single observation point is proved in simulation.

**Index Terms**—Partial discharge, on-line location, monitoring, electromagnetic time reversal (EMTR), transmission line, transmission line-matrix (TLM), network resilience.

## I. INTRODUCTION

AMONG all forms of energy, electricity plays a central role in the global challenge of climate change and the shift to clean growth. An increased amount of consumed electricity is expected in the transport, heating and service sectors. Electricity security is the power system's capability to withstand or cope with disturbance events or incidents producing abnormal system conditions, failures or outages of system components, with minimal service disruption [1]. Insulation degradation of cables in distribution and transmission networks produces effects ranging from temporary faults to complete black-out. Statistics indicate that more than 85% of equipment failures are related to insulation failure [2]. Insulation degradation is often caused by or accompanied by Partial Discharge (PD) events, which makes detecting and locating PDs an excellent 'early warning' indicator of impending cable failure. PDs start in insulation defects, usually formed during the manufacturing or installation process or in insulation deteriorated with age or by thermal/electrical over-stressing. Hence, the adoption of

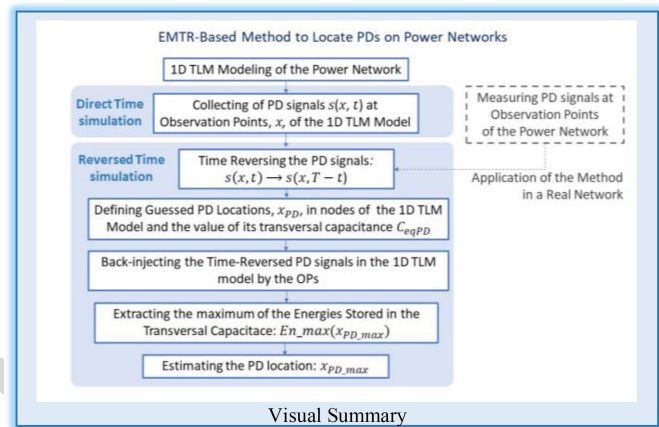
Manuscript received August 22, 2020; revised October 09, 2020; accepted October 15, 2020. This work was supported by the European Union's Horizon 2020 Research and Innovation Programme under the Marie Skłodowska-Curie Grant under Agreement 838681. (Corresponding author: A. Ragusa.)

A. Ragusa, H. Sasse, and A. Duffy are with the School of Engineering and Sustainable Development, De Montfort University, Leicester LE1 9BH, U.K. (e-mail: antonella.ragusa@dmu.ac.uk; hgs@dmu.ac.uk; apd@dmu.ac.uk).

F. Rachidi is with the Electromagnetic Compatibility Laboratory, Engineering School, École Polytechnique Fédérale de Lausanne, 1015 Lausanne, Switzerland (e-mail: farahd.rachidi@epfl.ch).

M. Rubinstein is with the Institute for Information and Communication Technologies, University of Applied Sciences and Arts Western Switzerland, 1401 Yverdon-les-Bains, Switzerland (e-mail: marcos.rubinstein@heig-vd.ch).

Digital Object Identifier 10.1109/LEMCPA.2020.3032465



on-line PD detection and location methods is the most effective solution for the condition monitoring of networks to prevent faults and supply interruption, leading to a better power quality, an increased customer satisfaction and an improvement of network resilience [3]. The on-line PD detection and location problem has been widely investigated in the literature [2]–[6]. Most on-line location methods are reflectometry or traveling wave-based techniques, using the principle that PD events generate electromagnetic waves that travel in either direction towards the cable ends. A measurement system at one end of the cable detects two pulses, the incident wave and the

### Take-Home Messages:

- The first results of the design of a method for the location of Partial Discharges (PDs) on power networks based on the innovative Electromagnetic Time Reversal (EMTR) theory and using a 1D TLM model of PD signals propagation are presented.
- The results demonstrate that EMTR theory is a promising mean to locate PDs using only one measurement point.
- The proposed technology, in the field of electromagnetic disturbance source-location identification, addresses the persisting question of the on-line diagnosis of power networks in order to improve their resilience.
- The EMTR-based method is able to locate PDs using only one measurement point, overcoming the complexities due to synchronization procedures of the existing reflectometry-based multi-end measurement methods.

44 reflected one from the other cable end. The delay between  
 45 these pulses allows an estimate of the PD location. Time  
 46 domain reflectometry (TDR) methods can only be used for  
 47 short cables because otherwise accuracy is lost due to atten-  
 48 uation and dispersion phenomena. Multi-end measurement  
 49 methods (ToA methods) [5] are used to address this problem,  
 50 but their implementation is difficult due to the complexity  
 51 in the synchronization procedure. Furthermore, ToA meth-  
 52 ods require a precise determination of the signal onset time,  
 53 which is highly sensitive to noise. Another major challenge  
 54 in accurately locating PDs is the presence of electromag-  
 55 netic interference (EMI), addressed using wavelet transform  
 56 techniques requiring significant computational effort [6].

57 This letter describes the first results of the design procedure  
 58 of a new method for the on-line location of PDs in dis-  
 59 tribution and transmission networks based on the innovative  
 60 theory of electromagnetic time reversal (EMTR) [7] and using  
 61 a 1D Transmission Line Matrix (TLM) method to model  
 62 the PD signal propagation. EMTR theory has already been  
 63 applied to the location of lightning strikes and faults in power  
 64 networks [8], [9] with significantly improved performance  
 65 compared to classical approaches, such as: applicability to  
 66 inhomogeneous and complex networks; robustness against the  
 67 presence of noise and a limited observation time window; use  
 68 of a single observation point. Moreover, the EMTR method  
 69 used to locate lightning can be considered a more general  
 70 case compared to ToA methods and is able to use information  
 71 about the wave shape of the lightning interference together  
 72 with the propagation time. EMTR has previously not been used  
 73 to locate incipient faults such as PDs which exhibit different  
 74 characteristics compared to solid faults. PD pulses are short  
 75 with significant frequency components of up to 1 GHz and  
 76 the accuracy of their location is influenced to a much greater  
 77 extent compared to classical faults by distortion phenomena  
 78 and by the presence of EMI. All these characteristics make  
 79 EMTR a good candidate technique to solve the highlighted  
 80 factors affecting the accuracy of PD location methods.

## 81 II. 1D TLM MODEL OF SIGNAL PROPAGATION

82 The propagation of PD signals in a lossless transmission line  
 83 formed by a single wire above a ground plane or a shielded  
 84 cable, represented by the equivalent circuit in Fig. 1, is  
 85 described by the Telegrapher's equations that give voltage,  
 86  $v(x, t)$ , and current,  $i(x, t)$  wave on the line as functions of  
 87 time  $t$  and distance  $x$  [10]:

$$88 \frac{\partial^2 v(x, t)}{\partial t^2} = \frac{1}{LC} \frac{\partial^2 v(x, t)}{\partial x^2} \quad (1.1)$$

$$89 \frac{\partial^2 i(x, t)}{\partial t^2} = \frac{1}{LC} \frac{\partial^2 i(x, t)}{\partial x^2} \quad (1.2)$$

90 where  $L$  and  $C$  are, respectively, the inductance and capaci-  
 91 tance (per unit-length) of the transmission line. The transmis-  
 92 sion line is thus characterized by a propagation speed,  $u$ , and  
 93 a characteristic impedance,  $Z_0$ , [10]:

$$94 u = \frac{\Delta x}{\Delta t} = \frac{1}{\sqrt{LC}}; \quad Z_0 = \sqrt{\frac{L}{C}} \quad (2)$$

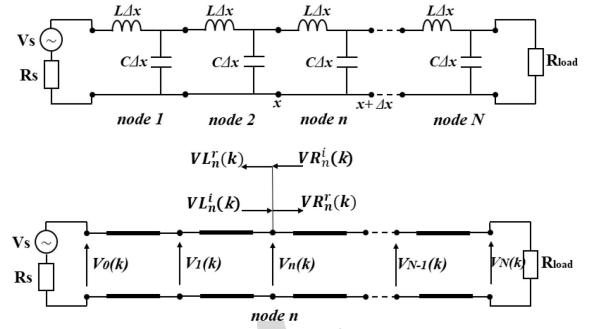


Fig. 1. Equivalent circuit of a line (top) and its TLM model (bottom).

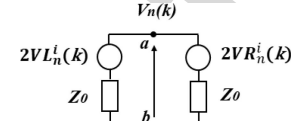


Fig. 2. Transmission line Thevenin equivalent.

95 Voltage and current waves are evaluated using the TLM  
 96 method, chosen for its flexibility, high efficiency, and its  
 97 numerical stability. It is a differential equation-based method  
 98 operating in time-domain, where the transmission line is dis-  
 99 cretized into a mesh of  $n$  segments, of length  $\Delta x$ , connected by  
 100 nodes as shown in Fig. 1. The wave pulses are scattered in the  
 101 nodes and propagate in the transmission lines, generating inci-  
 102 dent and reflected voltages/currents. The voltage at time-step  $k$   
 103 at the node  $n$ ,  $V_n(k)$ , evaluated by applying Millman's "Parallel  
 104 Generator" theorem to the Thevenin equivalent circuit of the  
 105 line shown in Fig. 2, and the node current,  $I_n(k)$  are:

$$106 V_n(k) = \frac{2VL_n^i(k)}{Z_0} + \frac{2VR_n^i(k)}{Z_0} \quad (3.1)$$

$$107 I_n(k) = \frac{V_n(k) - 2VR_n^i(k)}{Z_0} \quad (3.2)$$

108 where  $VL_n^i(k)$  and  $VR_n^i(k)$  are the incident voltages coming  
 109 respectively from the left and the right of node  $n$ . The reflected  
 110 voltages on the left,  $VL_n^r(k)$ , and on the right,  $VR_n^r(k)$ , of the  
 111 node are:

$$112 VL_n^r(k) = VL_n(k) - VL_n^i(k) \quad (4.1)$$

$$113 VR_n^r(k) = VR_n(k) - VR_n^i(k) \quad (4.2)$$

114 The voltage incident from the left of node  $n$  at time step  $k+1$   
 115 is the reflected into the right of node  $n-1$  at the time-step  $k$ ;  
 116 and the same considerations apply to the incident voltage on  
 117 node  $n$  coming from the right. In a node of the line where  
 118 a PD event occurs, an electromagnetic disturbance,  $V_{PD}$ , is  
 119 produced, and for the purpose of this illustration, it can be  
 120 represented with a double exponential equation [11]:

$$121 V_{PD} = V_0 \left( -e^{-\frac{t}{\tau_1}} + e^{-\frac{t}{\tau_2}} \right) \quad (5)$$

122 with  $V_0 = 0.1$  V,  $\tau_1 = 2$  ns,  $\tau_2 = 10$  ns. This voltage is  
 123 applied to one node of the TLM model, between points  $a$  and  
 124  $b$  of Fig. 2, and its propagation along the cable is evaluated  
 125 using eqs. (3-4).

### III. EMTR-BASED LOCATION METHOD

126

127 The EMTR-based method to locate PDs is derived from  
 128 the EMTR method to locate faults on power networks [9]. At  
 129 a point on the line, illustrated in Fig. 3, a PD event occurs.  
 130 To locate the PD source, the proposed EMTR-based method  
 131 is based on the following steps:

132 1. measurement of the PD-originated signals at observation  
 133 points (OPs) of the line, shown in Fig. 3;  
 134 2. simulation of the back-injection of the time-reversed PD  
 135 signals for different guessed PD locations (GPDs) using the  
 136 1D TLM model;

137 3. assessment of the PD location by evaluating the GPD  
 138 characterized by the highest energy concentration related to  
 139 the back-injected time-reversed PD signals.

140 The method is designed considering either two OPs or one  
 141 OP. To give the mathematical proof of the method, a Direct  
 142 Time (DT) simulation is run, during which a PD event occurs  
 143 at a node of the cable, producing the electromagnetic signal,  
 144  $V_{PD}$ , described by eq. (5). This propagates towards the cable  
 145 ends where the PD signals,  $s(t)$ , are recorded at the OPs, shown  
 146 in Fig. 3, in a specific time window,  $T$ . The recorded signals are  
 147 time-reversed and back injected, from the OPs, into the TLM  
 148 model of the line to run the Time Reversal (TR) simulations.  
 149 To make the argument of the time-reversed variables positive  
 150 during the TR simulations, a time delay equal to  $T$  is applied:

$$151 \quad \hat{t} = T - t \quad \text{with} \quad \bar{s}(\hat{t}) \quad \hat{t} \in [0, T] \quad (6)$$

152 For each TR simulation, a GPD is defined as a node of the  
 153 TLM model of the network that reproduces the transversal  
 154 impedance between the inner conductor and external shield of  
 155 the cable when a PD event occurs inside the insulator. A PD  
 156 event in a cavity within a dielectric can be modelled using the  
 157 well-known three-capacitor circuit model [12] shown in Fig. 4,  
 158 where  $C_a$  and  $C_b$  represent the capacitance in the dielectric  
 159 material in series with a defect and  $C_c$  is the defect capaci-  
 160 tance. The discharge event is represented by an instantaneous  
 161 change in the charging of the system capacitance, realized by  
 162 closing the switch in Fig. 4. The value of the defect capaci-  
 163 tance,  $C_c$ , can be evaluated by using the generalized PD model  
 164 described by Niemeyer [13]. According to this model, the  
 165 charges  $\pm q$  that represent the surface charge distribution in  
 166 the defect surface due to the voltage collapse,  $\Delta V_{PD}$ , caused  
 167 by the PD event, are given by:

$$168 \quad \pm q = \pm g \pi \varepsilon_0 d \Delta V_{PD} \quad (7)$$

169 where  $\varepsilon_0$  is the vacuum permittivity,  $d$  is the defect scale, i.e.,  
 170 the defect dimension parallel to the local background electric  
 171 field,  $g$  is a dimensionless proportionality factor accounting  
 172 for the charge distribution form, the defect geometry, and the  
 173 influence of the relative permittivity. The value of  $C_c$  can be  
 174 evaluated from (7):

$$175 \quad C_c = g \pi \varepsilon_0 d \quad (8)$$

176 For a generic defect type, shown in Fig. 4,  $g$  is given  
 177 by [12]:

$$178 \quad g(a/b, \varepsilon_r) = \frac{1}{2} \frac{a/d}{(a/b)^2} [1 + \varepsilon_r (K(a/b) - 1)] \quad (9)$$

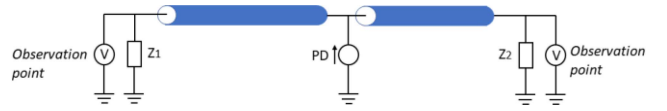


Fig. 3. Schematic representation of the line with a PD event along the cable and two OPs at the cable ends.

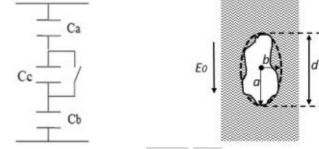


Fig. 4. Three-capacitor circuit model of PD (left) and a generic defect inside the insulation where PD occurs (right).

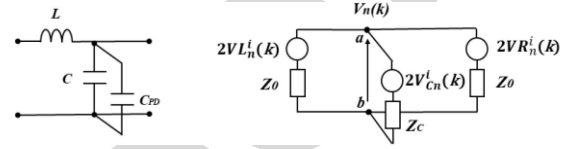


Fig. 5. TLM GPDL node with a capacitive stub (left) and the Thevenin equivalent circuit (right).

with  $\varepsilon_r$  the relative dielectric permittivity of the dielectric in  
 the vicinity of the defect,  $a$  and  $b$  defined in Fig. 4 and  $K(a/b)$   
 given by:

$$K(a/b) = \begin{cases} \cong 1 & a/b \ll 1 \\ 3 & a/b = 1 \\ \cong 4a/b & 1 < a/b < 10 \end{cases} \quad (10)$$

For a spherical void with  $d = 2a = 2b$  and  $K = 3$ , the  
 value of  $C_c$  is:

$$C_c = \pi \varepsilon_0 d \frac{1}{4} [1 + 2\varepsilon_r] \quad (11)$$

Then, in the TR simulations, the impedance at each GPD is  
 characterized by a capacitance  $C_{eqPD}$  given by the series of  $C_a$   
 and  $C_b$  with  $C_c$  short-circuited. In the TLM model, the value  
 of  $C_{eqPD}$  is realized, as shown in Fig. 5, using, in parallel with  
 the node transversal capacitance  $C$ , a stub capacitor [10],  $C_{PD}$ .  
 In the Thevenin equivalent circuit of the line, the GPD node  
 is shown in Fig. 5 where the stub capacitance is characterized  
 by an impedance,  $Z_c$ , given by:

$$Z_c = \Delta t / 2C_{PD} \quad (12)$$

In order to locate the PD source, at each GPD, the  
 Energy,  $E_n$ , stored in the transversal capacitance is evaluated  
 as follows:

$$E_{nGPDL} = \frac{1}{2} C_{eqPD} \sum_{i=1}^M V_i^2 \quad \text{with} \quad M = T/\Delta t \quad (13)$$

where  $V$  is the voltage at the node,  $M$  is the number of sam-  
 ples,  $\Delta t$  the sampling time and  $T$  the observation period. The  
 normalized value,  $E_{norm}$ , is then evaluated, for each GPD,  
 with respect to the maximum Energy in the GPDs:

$$E_{norm} = \frac{\frac{1}{2} C \sum_{k=1}^M V_{GPDL}^2(k)}{\frac{1}{2} C \sum_{k=1}^M V_{GPDL\_m}^2(k)} = \frac{\sum_{k=1}^M V_{GPDL}^2(k)}{\sum_{k=1}^M V_{GPDL\_m}^2(k)} \quad (14)$$

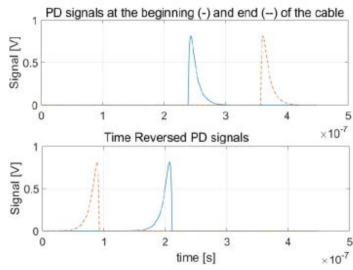


Fig. 6. PD signals measured at the two OPs in DT simulation with a PD source 40 m far from the left end of the cable and the Time Reversed signals.

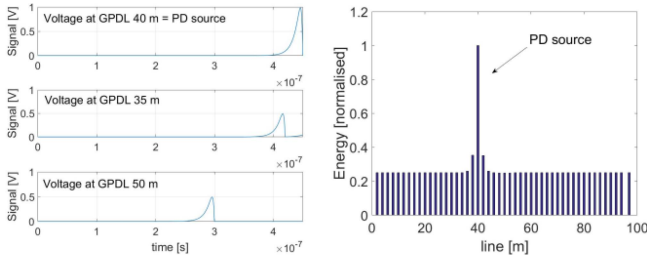


Fig. 7. Voltage at three GPDs and the energy in several GPDs in the TR simulation when 2 OPs are used, and the PD is 40 m from the line left end.

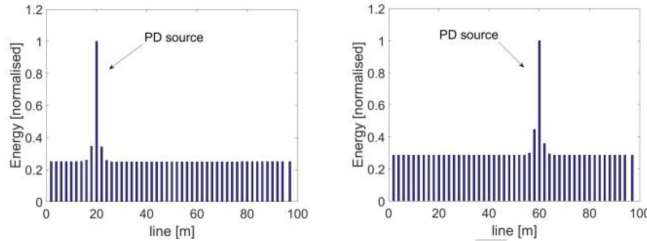


Fig. 8. Normalized energy in several GPD when PD source is 20 m and 60 m far from the left end of the cable when 2 OPs are used.

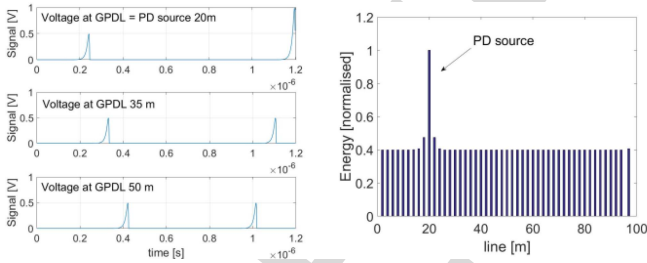


Fig. 9. Voltage in three GPDs and the Energy in several GPDs in the TR simulation when 1 OP is used, and the PD is 20 m from the line left end.

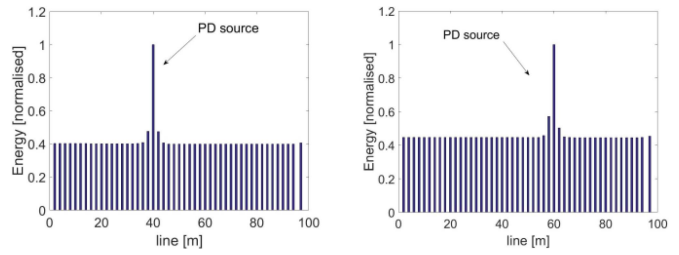


Fig. 10. Normalized energy in several GPDs when PD source is 40 m and 60 m far from the left end of the cable when 1 OP is used.

insulation and cross-sectional area of  $150 \text{ mm}^2$ , with characteristic parameters equal to  $L = 91.34 \text{ nH/m}$ ,  $C = 0.39 \text{ nF/m}$ , characteristic impedance  $Z_0 = 15.30 \Omega$  and propagation speed  $u = 1.675 \times 10^8 \text{ m/s}$ . The GPDL impedance in the TR simulations is evaluated using eqs (6)-(13). For an XLPE cable with  $\epsilon_r = 2.3$  and for a sphere defect with  $a = b = 1 - 5 \text{ mm}$ , the value of  $C_c \cong 10^{-13} - 10^{-14} \text{ F}$  and  $C_{PD} \cong 10^{-18} \text{ F}$ . The recording time  $T$ , when two OPs are used, must be equal to  $T = l/u = 0.6 \mu\text{s}$ , i.e., the propagation time along the cable, in order to measure the PD signals at both the OPs whenever the PD event occurs. Fig. 6 shows the PD signals measured at the OPs in the DT simulation, with a PD source 40 m away from the left end of the cable, and the corresponding time reversed signals. Fig. 7 shows the voltage at three GPDs and the normalized energy evaluated at several GPDs in the TR simulation. A GPDL was defined every 2 m along the cable. As the figure shows, the GPDL with the maximum energy is the PD source location. It can also be observed that the voltage at the GPDL that corresponds to the PD source is higher than the voltage at the other GPDs. This is because the back-injected signals add up in phase at the real PD location. Fig. 8 shows the results when the PD source is placed, respectively, 20 m and 60 m from the left end of the cable. The proposed method is also able to locate the PD source using only one OP. In this case, the recording time must be defined to measure at the OP the direct PD signal and some PD signal reflections from the other end of the cable. A value  $T = 2 \cdot l/u = 1.2 \mu\text{s}$  has been used. Fig. 9 shows the voltage at different GPDs when the PD source is 20m from the left end of the cable (where there is the OP) and the normalized energy in several GPDs. Fig. 10 shows the method results when the PD source is, respectively, 40 m and 60 m away from the left end of the cable. As the figures show, the method can locate the PD also using only one observation point.

## V. CONCLUSION AND FUTURE WORK

The letter proposes a new method for the on-line location of PD sources on power networks based on EMTR theory using a 1D TLM model of the PD signal propagation. An illustration of the method is provided and the ability of the method to locate PD events using only one observation point is demonstrated. The design of the method has been developed considering a simple system formed by a homogeneous Medium Voltage cable and using a lossless model of the transmission line. Future work includes the validation

204 The PD source is in the GPDL characterized by the  
205 maximum value of the Energy.

## IV. SIMULATION RESULTS

206  
207 To give an illustration of the proposed method, simula-  
208 tions have been performed based on the scheme in Fig. 3:  
209 that is, a transmission line formed of a homogeneous cable  
210 of length  $l = 100 \text{ m}$ , connected to impedances  $Z_1$  and  $Z_2$   
211 with  $Z_1 = Z_2 = 100 \text{ k}\Omega$  (representing the power transformers  
212 impedance at high frequency). The cable is an 11-kV alu-  
213 minium power cable, with Cross-Linked Polyethylene (XLPE)

259 of the method in complex network topologies (inhomogeneous  
 260 cables and branched networks) to introduce losses and analyze  
 261 the effect of this on the accuracy of the method to locate PDs.  
 262 Moreover, an analysis of the effect of the parameter  $K(a/b)$ ,  
 263 that defines the value of  $C_c$  in the GPDL, will be carried out  
 264 in order to verify if its value affects the behavior/profile of  
 265 the energy bar chart. This will potentially allow the method  
 266 to give information about the type, geometry and dimensions  
 267 of the defect where PD occurred in addition to only locating  
 268 its source.

## REFERENCES

- 270 [1] G. Fulli, F. Profumo, and E. Bompard, *Electricity Security in the*  
 271 *EU: Features and Prospects*, Joint Res. Centre, Brussels, Belgium,  
 272 Aug. 2018.
- 273 [2] S. Refaat and M. Sham, "A review of partial discharge detection, diag-  
 274 nosis techniques in high voltage power cables," in *Proc. IEEE Conf.*  
 275 *Compat. Power Electron. Power Eng.* Doha, Qatar, 2018, pp. 1–5.
- 276 [3] F. Auzanneau, "Wire troubleshooting and diagnosis: Review and per-  
 277 spectives," *Progr. Electromagn. Res. B*, vol. 49, pp. 253–279, Feb. 2013.
- 278 [4] M. S. Mashikian, R. Bansal, and R. B. Northrop, "Location and char-  
 279 acterization of partial discharge sites in shielded power cables," *IEEE*  
 280 *Trans. Power Del.*, vol. 5, no. 2, pp. 833–839, Apr. 1990.
- [5] C. C. Yü, M. N. K. H. Rohani, M. Isa, and S. I. S. Hassan, "Multi- 281  
 end PD location algorithm using segmented correlation and trimmed 282  
 mean data filtering techniques for MV underground cable," *IEEE Trans.* 283  
*Dielectr. Electr. Insul.*, vol. 24, no. 1, pp. 92–98, Feb. 2017. 284
- [6] A. M. Gaouda, A. El-Hag, T. K. Abdel-Galil, M. M. A. Salama, and 285  
 R. Bartnikas, "On-line detection and measurement of partial discharge 286  
 signals in a noisy environment," *IEEE Trans. Dielectr. Electr. Insul.*, 287  
 vol. 15, no. 4, pp. 1162–1773, Aug. 2008. 288
- [7] F. Rachidi *et al.*, *Electromagnetic Time Reversal—Application to* 289  
*Electromagnetic Compatibility and Power System*. Hoboken, NJ, USA: 290  
 Wiley, 2017. 291
- [8] G. Lugrin, N. Mora, F. Rachidi, M. Rubinstein, and G. Diendorfer, 292  
 "On the location of lightning discharges using time reversal of elec- 293  
 tromagnetic fields," *IEEE Trans. Electromagn. Compat.*, vol. 56, no. 1, 294  
 pp. 149–158, Feb. 2014. 295
- [9] S.-Y. He *et al.*, "Norm criteria in the electromagnetic time reversal tech- 296  
 nique for fault location in transmission lines," *IEEE Trans. Electromagn.* 297  
*Compat.*, vol. 60, no. 5, pp. 1240–1248, Oct. 2018. 298
- [10] C. Christopoulos, *The Transmission-Line Modeling Method—TLM*, 299  
 New York, NY, USA: Inst. Elect. Electron. Eng., 1995. 300
- [11] B. Sheng *et al.*, "Partial discharge pulse propagation in power cable 301  
 and partial discharge monitoring system," *IEEE Trans. Dielectr. Electr.* 302  
*Insul.*, vol. 21, no. 3, pp. 948–956, Jun. 2014. 303
- [12] N. Kartalović, D. Kovačević, and S. Milosavljević, "An advanced model 304  
 of partial discharge in electrical insulation," *Facta Universitatis Electron.* 305  
*Energetics*, vol. 24, no. 1, pp. 43–57, Apr. 2011. 306
- [13] L. Niemeyer, "A generalized approach to partial discharge modeling," 307  
*IEEE Trans. Dielectr. Electr. Insul.*, vol. 2, no. 4, pp. 510–528, 308  
 Aug. 1995. 309